Tree-Ring-Based Reconstruction of Precipitation in the Bighorn Basin, Wyoming, since 1260 A.D.

STEPHEN T. GRAY

Department of Botany, University of Wyoming, Laramie, Wyoming

CHRISTOPHER L. FASTIE

Department of Biology, Middlebury College, Middlebury, Vermont

STEPHEN T. JACKSON

Department of Botany, University of Wyoming, Laramie, Wyoming

JULIO L. BETANCOURT

Desert Laboratory, U.S. Geological Survey, and The University of Arizona, Tucson, Arizona

(Manuscript received 23 June 2003, in final form 2 March 2004)

ABSTRACT

Cores and cross sections from 79 Douglas fir (*Pseudotsuga menziesii*) and limber pine (*Pinus flexilis*) trees at four sites in the Bighorn Basin of north-central Wyoming and south-central Montana were used to develop a proxy for annual (June–June) precipitation spanning 1260–1998 A.D. The reconstruction exhibits considerable nonstationarity, and the instrumental era (post-1900) in particular fails to capture the full range of precipitation variability experienced in the past ~750 years. Both single-year and decadal-scale dry events were more severe before 1900. Dry spells in the late thirteenth and sixteenth centuries surpass both magnitude and duration of any droughts in the Bighorn Basin after 1900. Precipitation variability appears to shift to a higher-frequency mode after 1750, with 15–20-yr droughts becoming rare. Comparisons between instrumental and reconstructed values of precipitation and indices of Pacific basin variability reveal that precipitation in the Bighorn Basin generally responds to Pacific forcing in a manner similar to that of the southwestern United States (drier during La Niña events), but high country precipitation in areas surrounding the basin displays the opposite response (drier during El Niño events).

1. Introduction

Recent and ongoing droughts emphasize the importance of understanding precipitation variability in semiarid regions of western North America. Instrumental weather records form the basis for assessments of drought risk and drought mitigation plans in the region. Studies from throughout the world, however, demonstrate that the instrumental record is often insufficient for capturing the full range of precipitation variability possible in a given area (Cook and Evans 2000). Instrumental records rarely exceed 100 yr in length and provide a limited sample of possible single- and multiyear precipitation anomalies. Furthermore, instrumental records are inadequate for examining the low-frequency variability that may underlie short-term precipitation trends (Cayan et al. 1998). In most of western North America, only three to four significant decadal-scale wet–dry events have occurred over the last century, and these regimes may each result from different forcing mechanisms (Gedalof and Smith 2001; Villalba et al. 2001).

Ring widths from climatically sensitive trees provide a means for developing long-duration climate proxies that can extend beyond the instrumental record to encompass several centuries or even millennia (Fritts 1976). Tree rings yield continuous, precisely dated proxies of annual climate that are often highly replicable (Fritts 1976; Cook and Kairiukstis 1990). With proper sampling and analysis, tree rings preserve both high- and low-frequency climate variability (Cook et al. 1995).

In the Bighorn Basin region of north-central Wyoming and south-central Montana (Fig. 1), drought risks

Corresponding author address: Dr. Stephen T. Gray, Big Sky Institute, Montana State University, 106 AJM Johnson Hall, Bozeman, MT 59717.
E-mail: sgray@montana.edu

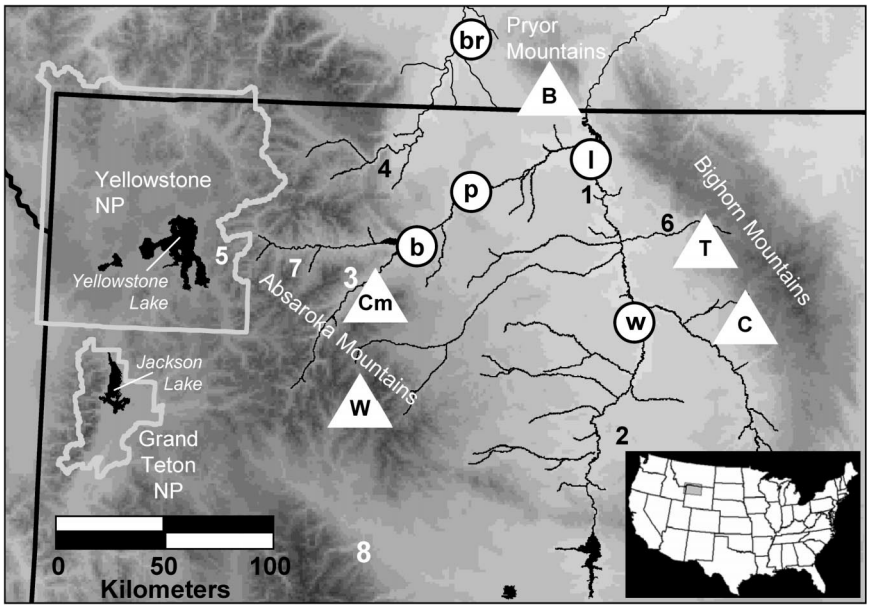

FIG. 1. Map of study area. White circles show locations of climate stations used to calibrate the tree-ring reconstruction models: **b** = Buffalo Bill Dam, Wyoming; **br** = Bridger, Montana; **l** = Lovell, Wyoming; **p** = Powell, Wyoming; **w** = Worland, Wyoming. Triangles mark individual study site locations: **B** = Bear Canyon; **Cm** = Carter Mountain; **C** = Cooks Canyon (sampled but not included in the final reconstruction, see section 3); **T** = Trapper Canyon; and **W** = Wood River. Major rivers and snow course/stream gauge locations are also shown: **1** = Bighorn River; **2** = Wind River; **3** = South Fork of the Shoshone River (gauge); **4** = Clark's Fork River (gauge); **5** = Sylvan Road (snow course); **6** = Shell Creek (gauge); **7** = Burroughs Creek (snow course); and **8** = South Pass (snow course).

are exacerbated by increasing demands for water coupled with changing economic needs and development patterns. Outdoor recreational activities such as hunting, fishing, skiing, snowmobiling, and boating are gradually replacing ranching and logging as the primary sources of income in the Bighorn Basin. Demands for recreational water, as well as water for fisheries and wildlife management, are often in conflict with demands for municipal and agricultural needs. While human populations in the Bighorn Basin were once concentrated in a few small, urban centers (<9000 inhabitants), a recent trend toward rural-residential or ''ranchette'' style development has led to increased construction in areas prone to wildfires and extended demands on groundwater resources.

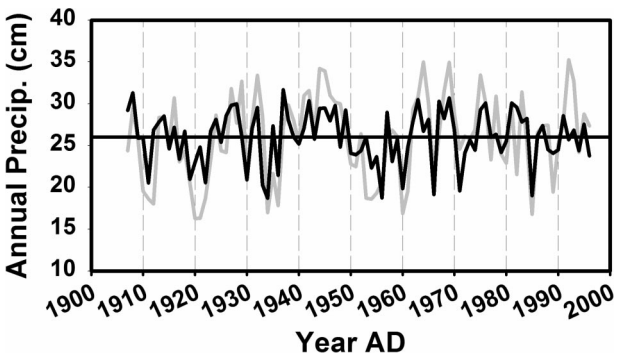

FIG. 2. Observed values (gray line) for previous Jun–current Jun total precipitation vs values predicted from the tree-ring reconstruction (black line) for the period from 1907 to 1998 A.D.

Here we present tree-ring-based reconstructions of annual (June–June) precipitation for the Bighorn Basin over the 1260–1998 A.D. interval and use these proxy records to assess the range of precipitation variability experienced in the region over the past 739 yr. More specifically, we examine the magnitude, frequency, and duration of past droughts in the Bighorn Basin and explore precipitation variability at interannual to multidecadal time scales. Although tree-ring-based drought reconstructions spanning 1700–1978 exist for all of North America (e.g., Cook et al. 1999), long (>700 yr), high-resolution precipitation records were not previously available for the Bighorn Basin.

In western North America as a whole, most of the precipitation variability at interannual to decadal and longer time scales is thought to originate in the Pacific basin as a result of interactions between the El Niño–Southern Oscillation (ENSO) and lower-frequency modes in the North Pacific (McCabe and Dettinger 1999). Recent studies, however, have pointed to the weakness of Pacific teleconnections in portions of the interior west, and the potential for complex interactions involving both the Pacific and Atlantic basins in the

development of widespread, persistent droughts. More specifically, based on an analysis of twentieth-century records from the neighboring upper Colorado River basin, Hidalgo and Dracup (2003) propose that linkages between Pacific basin variability and precipitation in the central Rockies may vary significantly in strength and sign over multidecadal periods. The instrumental record, however, provides only two such sign reversals. Enfield et al. (2001) and, more recently, McCabe et al. (2004) also suggest that slow changes in North Atlantic sea surface temperatures may affect the flow of warm-season moisture from the Gulf of Mexico to the central Rockies, thereby modulating the influence of the Pacific on droughts in Wyoming and Montana. In addition, a large portion of the Bighorn Basin's annual precipitation falls during the summer months as a result of convective thunderstorms (Martner 1986), producing a heterogeneous distribution of moisture throughout the region. Accordingly, we use the large sample of reconstructed precipitation values in these tree-ring proxy records to examine the potential role of remote forcing mechanisms versus local controls on Bighorn Basin hydroclimate.

2. Study area

The Bighorn Basin encompasses over 23 000 km^2 of mainly desert grasslands, sagebrush steppe, semiarid woodlands, and riparian corridors in north-central Wyoming and south-central Montana (Fig. 1). Elevations in the basin are as low as 1150 m, but with the Absaroka and Beartooth Ranges to the west, the Wind River Mountains to the southwest, and the Bighorn Mountains to the east, the area is almost completely surrounded by high ($>$4000 m) mountains. Two lower ($\sim$2700 m) ranges, the Pryor and Owl Creek Mountains, further enclose the north and south ends of the Bighorn Basin, respectively. Rainshadow effects thus persist across all seasons, making the basin relatively arid. The Bighorn River, which runs through the center of the basin, has its headwaters in the Wind River Mountains, some 50–75 km to the southwest. Major tributaries to the Bighorn River, including the Shoshone, Greybull, and Nowood Rivers, have their headwaters in the other mountains surrounding the basin.

Summers in the Bighorn Basin are warm (July average daily temperature = 20.4°C) with occasional high temperatures over 35°C (Martner 1986). January is the coldest month with an average daily temperature of −6.9°C. On average, meteorological stations in the Bighorn Basin receive 25.7 cm of mean annual precipitation (MAP). However, precipitation varies widely throughout the basin, with the lowest interior stations receiving as little as 16.1 cm MAP (Greybull, Wyoming; 1155 m). Sites at higher elevations on the eastern rim of the basin (e.g., Tensleep, Wyoming; 1463 m) can receive $>$33 cm MAP. Stations at equivalent elevations on the western edge of the basin (e.g., Cody, Wyoming; 1463 m; MAP = 23.7 cm) are generally drier due to rainshadow effects from the Absaroka and Beartooth mountain ranges located to the west.

The nearby Yellowstone Plateau receives its maximum precipitation in January as Pacific moisture is delivered to the area via winter storm tracks (Mock 1996). The high mountains surrounding the Bighorn Basin also receive significant snowfall in January, February, and March. In contrast, the Bighorn Basin experiences peak precipitation in the months of April, May, and June. During these months moisture from the Gulf of Mexico invades the Great Plains and is shunted into the Bighorn area by cutoff lows associated with upslope flows along the eastern front of the Rocky Mountains (Hirschboeck 1991; Mock 1996). In April and May, this moisture often falls as snow, especially along the western rim of the basin. In June, moisture is delivered through convective thunderstorms that originate in the mountains and later descend toward the basin floor, producing a heterogeneous rainfall distribution.

3. Data and methods

a. The Bighorn Basin tree-ring chronology network

We sampled trees at two sites in the western foothills (1600–2200 m) of the Bighorn and Pryor Mountains of north-central Wyoming and southern Montana and two sites in the lower elevations (2200–2600) of the eastern Absaroka Range (Fig. 1). All sites were characterized by poorly developed, rocky soils supporting open-canopy woodlands, and each site was near the lower to middle elevational range for the tree species sampled. We sampled limber pines (*Pinus flexilis*) at the two Absaroka Range sites and Bear Canyon, Montana, and Douglas fir (*Pseudotsuga menziesii*) at Trapper Canyon. We extracted at least two increment cores from all the living trees we sampled, and cores or cross sections were taken from available dead wood.

After mounting and progressively sanding to $>$400 grit, cores and sections were subjected to standard graphical dating methods (Stokes and Smiley 1968; Swetnam et al. 1985; Cook and Kairiukstis 1990). After rings in each series were measured to the nearest 0.001 mm, we used the COFECHA program (Holmes 1983) to confirm our dating by comparing ring-width measurements among all series within a site and among nearby sites. Dating could be verified for a total of 103 series among the four sites (Table 1). Interseries correlations were high at each site (r = 0.68–0.78), as were correlations between chronologies at neighboring sities (r = 0.36–0.76).

The Auto-Regressive Standardization (ARSTAN) program (Cook 1985) was used to detrend individual series with a negative exponential or linear spline to preserve climate-related variation at both high and low frequencies. All chronologies in this study contain significant autocorrelation at lags of 1–2 yr. Because such

TABLE 1. Descriptive statistics for the individual site chronologies.

Site name	Species	Elevation (m)	Time span (years A.D.)	Year SSS >0.85	Number of		Average series length (years)*	Interseries correlation
					Trees*	Series (radii)*		
Bear Canyon	*Pinus flexilis*	2000–2200	372–1998	1027	17	18	582.3	0.74
Carter Mountain	*Pinus flexilis*	2400–2600	1057–2000	1254	20	28	451.0	0.73
Trapper Canyon	*Pseudotsuga menziesii*	2000–2200	1250–1998	1250	21	30	557.1	0.78
Wood River	*Pinus flexilis*	2200–2600	1100–2000	1258	21	27	460.5	0.68

* Statistics for portion of chronology with subsample signal strength (SSS) > 0.85 (see Wigley et al. 1994).

autocorrelation is likely caused or amplified by biological factors (e.g., multiyear needle retention in conifers) rather than climate (Fritts 1976), we used a low-order autoregressive-moving-average (ARMA) filter within the ARSTAN program to remove this high-frequency persistence (Box and Jenkins 1970). As is generally the case in dendroclimatic studies, sample depth declines in the early portions of these chronologies (Table 1). Therefore, we used subsample signal strength (SSS) with a cutoff value of 0.85 (85% of common chronology signal retained) to assess replication through time at each site (Wigley et al. 1984).

b. Testing the climate–growth relationship

To determine the suitability of these chronologies for use in precipitation reconstructions, we first investigated the climate–growth relationship at the individual tree-ring sites using correlation analyses that compared ring widths to instrumental climate records obtained from the National Climatic Data Center (information online at http://www.ncdc.noaa.gov/oa/ncdc.html) and Historical Climatology Network (HCN; visit their Web site at http://www.ncdc.noaa.gov/oa/climate/research/ushcn/ushcn.html). All records in the HCN have been adjusted for measurement and location biases, and missing data have been estimated using data from neighboring stations (Easterling and Peterson 1995). Comparisons included ring-width index values versus monthly and seasonalized precipitation and temperature records from nearby meteorological stations and National Climatic Data Center state climate divisions. The divisional variables also included monthly and seasonal Palmer Drought Severity Index (PDSI) values (Palmer 1965; Alley 1984). Variables with lags of ± 1 yr were also examined.

Correlation analysis showed relationships between measures of local and regional moisture status and tree growth at all sites (Gray 2003). All sites showed significant ($p < 0.05$) correlations ranging from $r = 0.2$ to 0.5 with annualizations (e.g., August–July, October–September, etc.) of either divisional or individual station total precipitation. The Trapper and Bear Canyon chronologies were most strongly correlated with divisional PDSI for the Bighorn Basin during the month of June (Trapper, $r = 0.49$; Bear, $r = 0.28$). The Trapper and Bear Canyon chronologies were also significantly correlated with PDSI values for every month of the year and average annual PDSI values (Trapper, $r = 0.45$; Bear, $r = 0.27$). Growth at Carter Mountain and Wood River Canyon was correlated with divisional PDSI, but only for the months of May, June, and July ($r = 0.21$ to 0.29). The Carter Mountain and Wood River Canyon chronologies were, instead, most strongly correlated with divisional precipitation for the month of June (Carter, $r = 0.35$; Wood River, $r = 0.38$). All sites also showed significant negative correlations between tree growth and temperature for some portion of the year. However, with the exception of the relationship between

May temperature and tree growth at Trapper Canyon ($p < 0.001$; $r = -0.43$), these correlations were much weaker than those between tree growth and precipitation. Overall, these tests confirmed that tree growth at each site was most strongly related to moisture variability in the Bighorn Basin region, making the chronologies suitable for subsequent drought reconstructions.

c. Reconstructing regional precipitation from the Bighorn Basin composite chronology

We subjected all four chronologies to a principal components Analysis (PCA; Richman 1986) in order to extract the shared (presumably regional climatic) signal for the years 1260–1998 A.D., the period when all chronologies exceed SSS > 0.85. The first eigenvector (hereafter PC1) explained 51.3% of the variation in tree growth among the chronologies (eigenvalue = 2.1) and showed positive loadings between 0.41 and 0.56 at all sites. The second eigenvector (hereafter PC2) explained an additional 26% of the variance (eigenvalue = 1.1) and was also retained for further analysis.

Response functions (Fritts 1976) comparing the ring-width PCs against measures of Bighorn Basin climate showed a moderate relationship ($r^2 > 0.3$) between PC1 and various precipitation and drought indices for the Bighorn Basin. PC1 was most strongly related ($r^2 = 0.42$) to previous June through present year's June (J–J) total precipitation averaged among the five longest HCN records from stations nearest the tree-ring sites (Fig. 1: Worland, Lovell, Powell, and Buffalo Bill Dam, Wyoming; and Bridger, Montana). To verify this relationship and develop a transfer function allowing estimation of J–J precipitation predating the instrumental record, we divided the period of time common to both tree rings and instrumental precipitation data (1907–96) into half-sample subsets by grouping early (1907–51) and late (1952–96) years. Simple linear equations describing the relationship between PC1 of late period ring-growth and late period J–J precipitation were developed and then verified against early period data. Validation statistics indicated that the model performed well in estimating precipitation values not included in the calibration dataset (Table 2). The model explained ~44% of the variance in the verification period and estimated the mean of J–J precipitation well. Model predictions of precipitation standard deviation were lower than observed values. However, such discrepancies are common in dendroclimatic reconstructions because of limitations imposed by tree physiology (Fritts 1976). The two subsets were then recombined and a final reconstruction model was calibrated on the full 1907–96 record ($r^2 = 0.42$). An additional model incorporating ring growth from a fifth site near Tensleep, Wyoming (Fig. 1), improved the total variance explained by 6%, but was rejected based on a 45% reduction in the length of the reconstruction. Comparisons of PC2 and Bighorn Basin climate showed only a weak, inverse relationship ($r^2 = -0.18$) to May temperature. Models combining PC1 and PC2 as predictors of basin climate explained less of the variance than models using PC1 alone, as did models using individual site chronologies and subsets of site chronologies as predictors.

TABLE 2. Model calibration and verification statistics for the reconstruction of previous Jun–current Jun total precipitation in the Bighorn Basin region.

	Calibration dataset (1952–96)		Verification dataset (1907–51)	
r	0.64		0.66	
r^2	0.41		0.44	
r^2 adj	0.39			
RE*			0.44	
Sign test (agree/disagree)	40/5		39/6	
	Observed	Reconstructed	Observed	Reconstructed
Mean (cm)	26.3	26.3	25.7	26.7
Std dev (cm)	4.8	3.1	5.0	3.1

* Reduction of error statistic (RE). Posiive values of RE demonstrate that the regression model is a better predictor of precipitation than the mean of the calibration dataset (Fritts 1976).

d. Spectral properties of the Bighorn Basin precipitation reconstruction

We used a multitaper method (MTM) analysis (Mann and Lees 1996) to examine the frequency characteristics of the Bighorn Basin precipitation reconstruction. MTM provides a robust means for separating the noise and signal components of climatic time series, particularly in datasets that may contain both periodic and quasi-periodic behavior. The use of MTM does not rely on a priori assumptions concerning the structure of the time series, and the method has been successfully employed in a number of paleoclimatic studies. Our analysis used $5 \times 3\ \pi$ tapers and a red noise background.

e. Exploring the influence of Pacific basin variability on Bighorn Basin precipitation

In order to examine the role of Pacific forcing in Bighorn Basin regional precipitation variability, we first compared instrumental records of precipitation with values of the Southern Oscillation index (SOI; November–March) obtained from the University of East Anglia's Climatic Research Unit (information online at http://www.cru.uea.ac.uk/cru/data/soi.htm) and values of the Pacific decadal oscillation index (PDO; November–March) from Mantua et al. (1997). We then compared our annual precipitation reconstruction against reconstructed indices of the SOI and PDO provided by Stahle et al. (1998) and Biondi et al. (2001), respectively. The PDO reconstruction spans 1661–1992, while the SOI

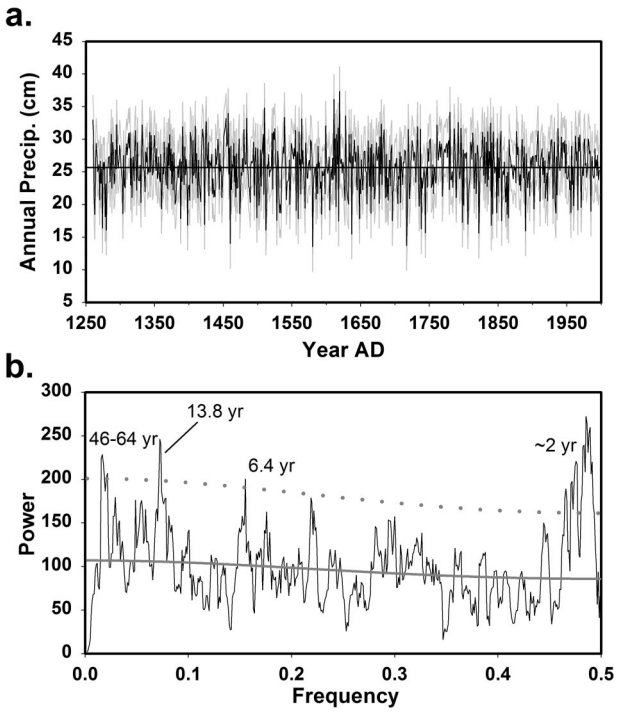

FIG. 3. (a) Reconstructed annual Bighorn Basin precipitation (previous Jun–current Jun) for the period 1260–1998 A.D. (black lines). The 95% confidence band (gray lines) was calculated from the root-mean-squared error estimates of the regression model for the full 1907–96 calibration period (Jain et al. 2002). The black horizontal line at 26.1 cm depicts the long-term mean. (b) Multitaper method spectra for the full Bighorn Basin precipitation reconstruction. The dotted gray line shows the 95% confidence level and the solid gray line shows the red noise background threshold.

reconstruction covers 1706–1977. Both reconstructions are based on tree-ring series from the southwestern United States and Mexico. The SOI reconstruction also includes tree-ring series from Indonesia. Both the SOI and PDO proxies were chosen over other available reconstructions (e.g., Cole et al. 2002; Gedalof and Smith 2001) based on the combination of high instrumental variance explained and large networks of predictor chronologies they provide.

4. Results

a. Reconstructed annual precipitation since 1260 A.D.

The full reconstruction of J–J precipitation (Fig. 3a) shows that the magnitude of the worst single-year drought events in the twentieth century (1934 and 1956) was likely equaled or exceeded on numerous occasions in the preceding seven centuries. The twentieth-century portion of the record contains just 2 of the 37 most severe drought years (lowest 5% of precipitation values) in the time series (Table 3). In contrast, the nineteenth century includes nine. At the 0.25-quantile level dry years are more equitably distributed throughout the record with the twentieth century having 18 drought years versus 21–29 yr for other centennial periods. Still the twentieth century appears to have relatively few severe drought years. The twentieth century also lacks extreme wet events such as those seen in the early seventeenth century (Fig. 3a).

TABLE 3. Driest (0.05 quantile) years for the 1260–1998 A.D. period based on the Bighorn Basin composite reconstruction. Years are further divided into three groups reflecting the 0.015, 0.035, and 0.05 quantile levels of the reconstruction. Two twentieth-century extreme dry years are shown in bold.

Quantile	Yr	Quantile	Yr	Quantile	Yr
<0.015	1274	<0.035	1388	<0.05	1263
	1280		1398		1278
	1460		1423		1304
	1512		1528		1474
	1580		1559		1499
	1637		1618		1534
	1717		1648		1593
	1738		1696		1665
	1744		1798		1842
	1822		1806		1848
	1840		1855		1863
	1890		1865		**1934**
					1956

In addition to interannual and multiyear variability, the MTM analysis shows that reconstructed precipitation in the Bighorn Basin varies significantly in the decadal (~14 yr) band (Fig. 3b). With the exception of the 1950s event, decadal-scale droughts in the twentieth century were of moderate magnitude compared to events in the preceding 600+ years, and the last four decades were free from extended (>10 yr) dry periods (Fig. 4a). With an average of 23.7 cm of annual precipitation, the 1952–61 interval was only the 28th driest 10-yr period in the reconstruction (Table 4). Earlier drought periods such as those from 1262 to 1281 and 1579 to 1598 averaged similarly low precipitation amounts for 20 yr. The reconstruction also shows pronounced variability at multidecadal (46–64 yr) time scales (Fig. 3b). The twentieth century, however, lacks any multidecadal dry anomalies (Fig. 4b). Portions of the record including roughly 1260–1300, 1360–1410, 1570–1605, 1685–1755, and 1845–1905 are notable because average precipitation during these periods falls almost 0.5 standard deviations below the long-term mean for 35 to 70 yr.

b. Links between Pacific basin variability and Bighorn Basin precipitation

Based on comparisons of instrumental precipitation records with observations of the Southern Oscillation index, Bighorn Basin climate shows a significant negative correlation ($r = -0.30$; $p < 0.01$) with conditions in the tropical Pacific (Fig. 5a). In particular, instrumental records show that dry (wet) events in the Bighorn Basin tend to coincide with strong La Niña (El Niño) conditions. The Bighorn Basin drought of the 1950s, for example, occurred during a series of strong La Niña

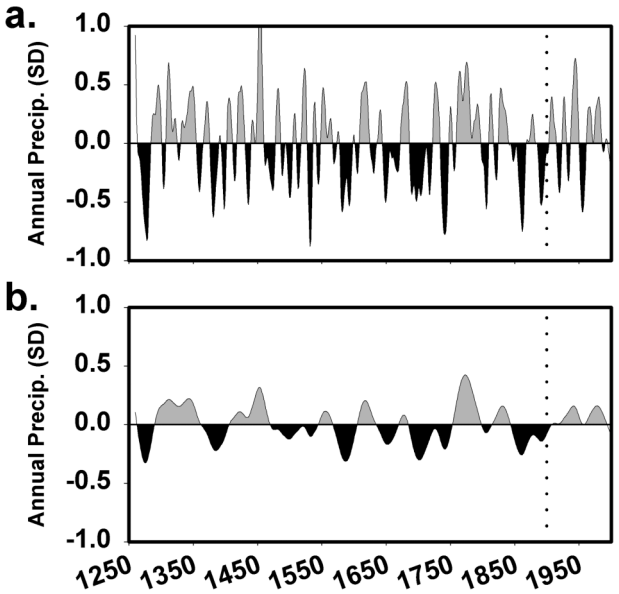

FIG. 4. (a) Reconstructed Bighorn Basin precipitation (previous Jun–current Jun) smoothed with a 14-yr cubic spline to highlight the dominant mode of decadal variability shown in Fig. 3b. The black horizontal line at 26.1 cm depicts the long-term mean. Periods of above average precipitation are shown in gray while periods of below average precipitation are shown in black. The vertical dotted line crosses at 1900. (b) As in (a) but smoothed with a 50-yr cubic spline to highlight the dominant modes of multidecadal variability.

years, while wet events around 1910–17, the 1940s, 1983, and 1992 coincided with strong El Niños. As depicted by instrumental records of the PDO index (Fig. 5b), conditions in the North Pacific appear to have little influence on interannual precipitation variability in the Bighorn Basin ($r = 0.06$; $p = 0.59$). However, the 1950s drought does coincide with a strong, extended cool period in the North Pacific, while a wet period in the 1940s occurred during a warm phase of the PDO.

Comparison of our reconstructed precipitation values with the Stahle et al. (1998) SOI proxy (Fig. 5c) suggests a consistent La Niña–Bighorn Basin drought link prior to the instrumental period. As in the 1950s, severe droughts in the 1860s, early 1800s, and 1715–20 coincided with extended periods where the proxy record shows warm conditions in the tropical Pacific. According to the Biondi et al. (2001) PDO reconstruction, prior to the twentieth century, several persistent Bighorn Basin droughts (e.g., 1860s and 1740s) coincided with warm phases in the North Pacific. On the other hand, wet periods in the 1830s and 1680s occurred during similar positive PDO conditions.

5. Discussion

a. Drought history of the Bighorn Basin

The network of four new tree-ring chronologies presented in this paper provides a well-replicated, statistically verified, and long-duration proxy for Bighorn Basin moisture variability. Large sample sizes and the conservative cutoff dates for use of individual chronologies in the reconstruction maximize the precipitation signal through even the early portions of the proxy record. In addition, the use of long segments (Table 1) facilitates comparisons between different periods in the reconstruction (Cook et al. 1995).

These records, in turn, provide a long-term perspective from which to evaluate twentieth-century precipitation variability. The 1950s event was, undoubtedly, an extreme drought. With reconstructed annual precipitation averaging only 23.7 cm from 1952 to 1961, the region experienced a deficit of nearly one year's average precipitation (26.1 cm) over this 10-yr period. This drought and the 1930s event are used as ''worst-case scenarios'' for drought planning and mitigation efforts in this area (Wyoming Water Development Commission 2003). However, the proxy record shows that these worst-case scenarios for twentieth-century drought were likely not the most extreme dry events in the previous seven centuries.

Two droughts in the preinstrumental period stand out for their severity and duration. The single driest event over the last seven centuries occurred from 1262 to 1281 (Figs. 4a,b; Table 4). While this event happened during the earliest years of the reconstruction, when sample depth was limited, several features of the proxy record lend credence to the reconstructed magnitude of this late thirteenth century drought. The proxy record at this point still includes a total of 26 series from four sites, and trees from all of these sites show a downturn in growth during these years. This portion of the record also includes samples from two tree species (*Pseudo-*

TABLE 4. Driest 10-, 15-, and 20-yr periods in the 1260–1998 A.D. proxy record, based on inferred MAP over the respective intervals. The driest periods in the twentieth century are shown for comparison.

Driest 10-yr period	Rank	MAP (cm)	Driest 15-yr period	Rank	MAP (cm)	Driest 20-yr period	Rank	MAP (cm)
1738–47	1	22.4	1580–94	1	23.3	1262–81	1	23.6
1272–81	2	22.6	1267–81	2	23.4	1579–98	2	23.7
1735–44	3	22.6	1268–82	3	23.4	1263–82	3	23.8
1271–80	4	22.8	1734–48	4	23.4	1261–80	4	23.9
1273–82	5	22.9	1579–93	5	23.5	1580–99	5	23.9
—	—	—	—	—	—	—	—	—
1951–60	28	23.7	1948–62	68	24.5	1917–36	149	25.0

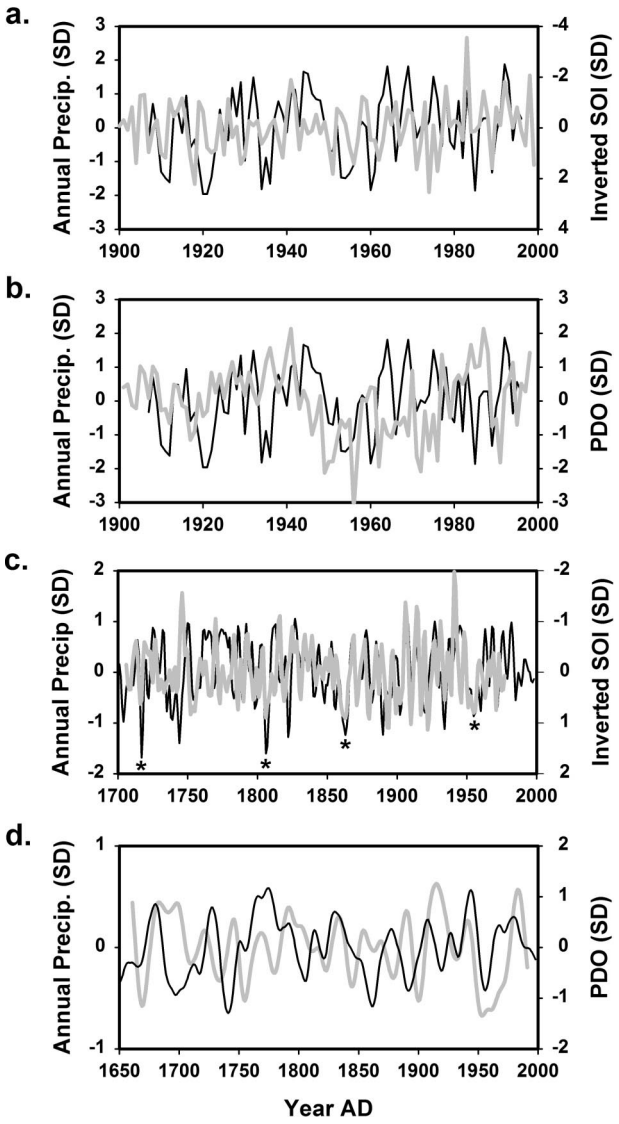

FIG. 5. (a) Instrumental values for Bighorn Basin annual (Jun–Jun) precipitation vs the SOI (information online at http://www.cru.uea.ac.uk/cru/data/soi.htm). Both precipitation and SOI values have been converted to standard deviation (SD) units, and the inverse SOI is shown for ease of comparison; $R = -0.30$; $p < 0.01$. (b) Same as in (a) but for the Pacific decadal oscillation index (Mantua et al. 1997); $R = 0.06$; $p = 0.59$. (c) As in (a) but for reconstructed Bighorn Basin precipitation (black line) and reconstructed SOI values [gray line; Stahle et al. (1998)]. Stars highlight periods where strong La Niñas (positive SOI) and severe Bighorn Basin drought coincide. Series were smoothed with a 5-yr cubic spline to highlight the dominant mode of SOI variability. (d) As in (c) but for a reconstructed PDO (Biondi et al. 2001). Series were smoothed with a 20-yr cubic spline to highlight the dominant mode of PDO variability.

tsuga menziesii and *Pinus flexilis*), minimizing the possibility that nonclimatic factors (e.g., insect outbreaks) were responsible for the decline in growth. During this 20-yr period, mean annual precipitation in the Bighorn Basin dropped to only 23.6 cm (versus the 26.1-cm long-term average). This period also encompasses four of the driest single years (1263, 1274, 1278, and 1280) in the proxy record (Table 3). Few comparable records of moisture variability exist for this interval. However, of those records from the western United States and Great Plains that span this period, almost all indicate severe, multidecadal drought at this same time (Woodhouse and Overpeck 1998). In particular, tree-ring chronologies from Nebraska, New Mexico, the Great Basin, and northeastern Utah show marked decreases in tree growth at or near this time (Grissino-Mayer 1996; Hughes and Graumlich 1996; Woodhouse and Overpeck 1998). Other proxies, including Nebraska Sand Hills eolian activation records (Muhs et al. 1997) and archeological data from the Southwest and Great Plains, document this drought (Dean 1994; Woodhouse and Overpeck 1998).

A second notable drought occurred during the late sixteenth century. Again, mean annual precipitation in the Bighorn Basin reconstruction dropped by almost 3 cm over the period from 1580 to 1594 (Table 4). Unlike the thirteenth-century drought, ample proxy records exist to help describe the spatial and temporal extent of this event. In a summary analysis of tree-ring chronologies spanning the late sixteenth century, Stahle et al. (2000) found strong evidence for this same drought extending from the southwestern United States and northern Mexico through the Rocky Mountains. Using an exceptionally long and well-replicated tree-ring chronology from western New Mexico, Grissino-Mayer (1996) suggested that this drought was the most severe in that region over the past 2000 yr. Based on tree-ring reconstructions of Colorado River flow at Lees Ferry, Arizona, Stockton and Jacoby (1976) estimated 1579–98 to be the driest two decades between 1520 and 1961 in the upper Colorado River basin. Furthermore, both tree-ring and documentary evidence show that this drought extended into the Carolinas and lower Mississippi Valley (Stahle et al. 2000). Not only were the thirteenth- and sixteenth-century droughts more severe than the 1950s event in the Bighorn Basin, but they were at least as widespread as the 1950s drought.

Additional severe, prolonged (>20 yr) droughts occurred in the fourteenth and seventeenth centuries (Table 4; Fig. 4b). These droughts, combined with the thirteenth- and sixteenth-century megadroughts, suggest that >20 yr dry events were common features of Bighorn Basin climate before ~1750. After the mid-eighteenth century, however, the proxy record contains only one such >20 yr drought (1850s and 1860s), indicating a fundamental change in Bighorn Basin precipitation regimes from a mode characterized by persistent, alternating multidecadal wet/dry events to one of decadal and higher frequency variability. Conditions after ~1750 were generally wetter than the long-term average (Fig. 4b). This may be especially true for the twentieth century. The driest 20-yr period (1917–36) from 1900 to 1998 ranks as only the 149th driest 20-yr period in the entire reconstruction (Table 4).

b. Links between the Pacific Ocean and Bighorn Basin climate

In general, the Bighorn Basin follows a climatic pattern like that of the southwestern United States, namely drier (wetter) during cool phase (warm phase), La Niña (El Niño) events (Figs. 5a,c). During the 1950s and 1860s, for example, persistent La Niña conditions brought severe drought to the southern Rockies and Great Plains (Cole et al. 2002). As seen in the instrumental record and our proxy reconstruction (Fig. 4a), these droughts also extended northward into the Bighorn Basin region. The coherency of several other major drought events in our reconstruction with severe dry events across the western United States (e.g., late thirteenth and sixteenth centuries) also points to remote forcing of precipitation anomalies in the Bighorn Basin. However, as measured by the Southern Oscillation index, the tropical Pacific explains little (~10%) of the interannual variability in either the observed or reconstructed records of Bighorn Basin precipitation.

This weak relationship between Bighorn Basin precipitation and the El Niño–Southern Oscillation may in part be a product of the annual (June–June) nature of our reconstruction. ENSO teleconnections in the western United States are generally strongest over the winter months (Cayan et al. 1999). Other remote forcing factors may also control the strength of ENSO–Bighorn Basin teleconnections. In particular, links between the tropical Pacific and precipitation in the western United States are thought to be modulated by decadal-scale variability in the North Pacific (Cole and Cook 1998; McCabe and Dettinger 1999). Strong negative PDO conditions from 1946 to 1976 (Fig. 5b), for example, may have amplified the 1950s La Niña–induced drought (Cole et al. 2002), but the PDO does not necessarily translate into wet or dry conditions for the Bighorn Basin. In fact, strong, negative PDO regimes in the early 1900s and late 1600s to early 1700s coincided with dry periods in the Bighorn Basin (Fig. 5d). Because of the uncertainties inherent in every proxy record (e.g., limited variance explained), these comparisons between reconstructed PDO and reconstructed precipitation must be interpreted cautiously, but our findings appear to support Hidalgo and Dracup's (2003) proposal that Pacific–central Rockies teleconnections may vary in strength and sign over decadal and longer time scales.

Enfield et al. (2001) suggest that multidecadal modes in the North Atlantic also play a role in western U.S. precipitation variability, particularly over the summer months, by modulating Pacific–western North America teleconnections and producing anomalous geopotential heights over the intermountain West region. A warm period in the North Atlantic from roughly 1930 to 1960 coincides with both the 1930s and 1950s droughts in the Bighorn Basin, but this period also features a relatively wet interval (e.g., 1940s). As suggested by McCabe et al. (2004), development of severe, prolonged drought conditions that span multiple seasons and years in the western United States is likely tied to complex interactions between Pacific and North Atlantic modes. McCabe et al. (2004) propose that, when coupled with cool conditions in the North Pacific, warm conditions in the North Atlantic tend to produce severe, regional- to subcontinental-scale droughts centered over the southwestern United States (e.g., 1950s; Fig. 6a). A warm North Atlantic coupled with a warm or neutral North Pacific, on the other hand, increases the likelihood of widespread drought centered over Wyoming, Montana, and the southern Canadian Rockies (Fig. 6b). The proxy records of North Atlantic multidecadal variability needed to fully evaluate these Atlantic–Pacific interactions are currently lacking (Gray et al. 2003). However, similar patterns of Southwest versus northern Rockies–centered drought have been observed in gridded precipitation reconstructions for the coterminous United States (Fye et al. 2003).

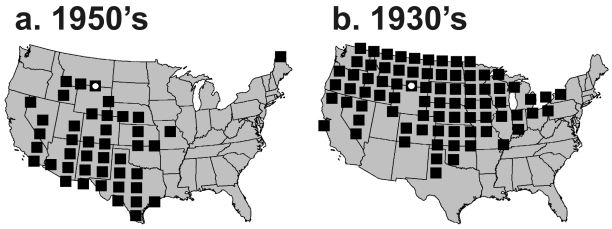

FIG. 6. (a) Spatial distribution of the 1950s (1946–57) drought from Fye et al. (2003). Areas with average Palmer Drought Severity Index < -1 for the period are shown in black, and the approximate location of the Bighorn Basin is outlined in white. (b) As in (a) but for the 1930s drought (1929–40).

In contrast, precipitation in the mountains surrounding the Bighorn Basin shows a moderate ($r \sim 0.5$) response to Pacific forcing in a manner similar to that of the northwestern United States (Table 5; Figs. 7a, b). More specifically, low snowpack and low runoff events in the higher elevations tend to occur during El Niño episodes and warm phases of the PDO (Cayan et al. 1999). This is particularly true for the high Absaroka and Beartooth Mountains and the Yellowstone Plateau (Graumlich et al. 2003). Such decoupling of high-elevation and lowland precipitation regimes is common throughout the Central Rocky Mountain region (Woodhouse 2001). This complicates our practical understanding of drought in these areas because much of the water for industry, irrigation, and domestic use originates as high-elevation snowpack, while soil moisture related to range production, vegetation stress, and wildland fuel–moisture results from local precipitation. In many cases, streamflow and reservoir storage originating from high-country snow may offset droughts in the lowlands. However, because these analyses show that lowland droughts in the Bighorn Basin may occur during North Pacific regimes that favor low mountain snowpack (e.g., positive PDO), this may not be the case for every drought event.

TABLE 5. Results of correlation analyses comparing snow course measurements and mean annual streamflows for high-elevation areas surrounding the Bighorn Basin with instrumental SOI and PDO index values. All correlations are significant at $p < 0.05$. See Fig. 1 for locations. MAF: mean annual flow from stream gauging station; SWE: snow water equivalent from snowcourse data.

Location	Record length	Variable	Correlation with PDO	Correlation with SOI
Clark's Fork River	1922–2001	MAF	−0.39	0.40
South Fork, Shoshone River	1957–2001	MAF	−0.46	0.39
Sylvan Road snow course	1937–2001	Apr SWE	−0.53	0.52
Shell Creek	1957–2001	MAF	−0.38	0.12
Burroughs Creek	1949–2001	Apr SWE	−0.35	0.41
South Pass snow course	1940–2001	Mar SWE	−0.41	0.33

6. Conclusions

Tree-ring records of Bighorn Basin drought spanning the last ~750 years show that twentieth-century instrumental records underestimate the severity of droughts this area has experienced. In particular, dry events of >20 yr were common prior to the 1750s. Single- and multiyear droughts regularly surpassed the severity and magnitude of the ''worst-case scenarios'' presented by the 1930s and 1950s droughts. Overall, the climate of the twentieth century was relatively wet compared to what this area has experienced in the past.

Because of complex topography and the delivery of substantial summer rainfall by convective thunderstorms, local processes undoubtedly control a portion of precipitation variability in the Bighorn Basin, especially at interannual time scales. However, the coincidence of several major Bighorn Basin droughts with persistent La Niña events and with droughts in the northern and southern Rockies points to remote forcing of Bighorn Basin hydroclimate. As emphasized by the occurrence of strong, persistent (>10 yr) moisture anomalies in the basin with both positive and negative modes of the Pacific decadal oscillation, controls on decadal-scale precipitation variability are still poorly understood in the central Rockies.

Links between Pacific modes and high-elevation precipitation are usually different than for low-elevation precipitation in the Bighorn Basin region. Specifically, lowland precipitation in the basin generally responds to Pacific forcing in a manner similar to that of the southwestern United States. The high country surrounding the Bighorn Basin typically displays the opposite response (dry during El Niño) to ENSO and ENSO-like modes. A more complete understanding of drought variability in the Bighorn Basin and other regions of the interior West will require coupled studies of high-elevation and lowland precipitation using both instrumental and proxy records.

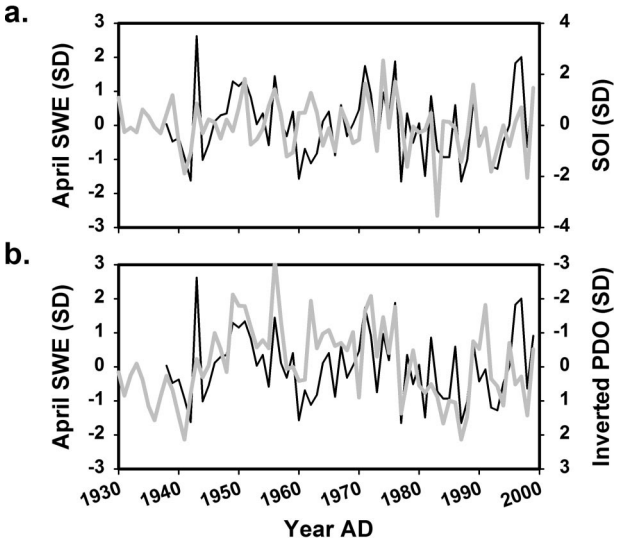

FIG. 7. (a) Comparison of observed 1 Apr snow water equivalent (SWE) values for the Sylvan Road snow course (black line) against instrumental values for the SOI (gray line; http://www.cru.uea.ac.uk/cru/data/soi.htm). The Sylvan Road snow course is located in the South Fork of the Shoshone River watershed near the eastern boundary of Yellowstone National Park (Fig. 1). (b) As in (a) but for the instrumental PDO index (Mantua et al. 1997).

Acknowledgments. This work was supported by the National Science Foundation, U.S. Geological Survey, Wyoming Water Development Commission, and University of Wyoming–National Park Service Research Station.

REFERENCES

Alley, W. M., 1984: The Palmer Drought Severity Index: Limitations and assumptions. *J. Climate Appl. Meteor.,* **23,** 1100–1109.

Biondi, F., A. Gershunov, and D. R. Cayan, 2001: North Pacific decadal climate variability since 1661. *J. Climate,* **14,** 5–10.

Box, G. E. P., and G. M. Jenkins, 1970: *Time Series Analysis: Forecasting and Control.* Holden-Day, 553 pp.

Cayan, D. R., M. D. Dettinger, H. F. Diaz, and N. E. Graham, 1998: Decadal variability of precipitation over western North America. *J. Climate,* **11,** 3148–3166.

——, K. T. Redmon, and L. G. Riddle, 1999: ENSO and hydrologic extremes in the western United States. *J. Climate,* **12,** 2881–2893.

Cole, J. E., and E. R. Cook, 1998: The changing relationship between ENSO variability and moisture balance in the continental United States. *Geophys. Res. Lett.,* **25,** 4529–4532.

——, J. T. Overpeck, and E. R. Cook, 2002: Multiyear La Niña events

and persistent drought in the contiguous United States. *Geophys. Res. Lett.,* **29,** 1647, doi:10.1029/2001GL013561.

Cook, E. R., 1985: A time-series analysis approach to tree-ring standardization. Ph.D. dissertation, The University of Arizona, Tucson, AZ, 171 pp.

——, and L. A. Kairiukstis, 1990: *Methods of Dendrochronology—Applications in the Environmental Sciences.* Kluwer Academic, 394 pp.

——, and M. Evans, 2000: Improving estimates of drought variability and extremes from centuries-long tree-ring chronologies: A PAGES/CLIVAR example. *CLIVAR Exchanges,* Vol. 5, No. 1, *PAGES Newsletter,* Vol. 8, No. 1, International CLIVAR Project Office, Southampton, United Kingdom, 10–12.

——, K. R. Briffa, D. M. Meko, D. A. Graybill, and G. Funkhouser, 1995: The ''segment length curse'' in long tree-ring chronology development for palaeoclimatic studies. *The Holocene,* **5,** 229–237.

——, D. M. Meko, D. W. Stahle, and M. K. Cleaveland, 1999: Drought reconstructions for the continental United States. *J. Climate,* **12,** 1145–1162.

Dean, J. S., 1994: The Medieval Warm Period on the southern Colorado Plateau. *Climatic Change,* **26,** 225–241.

Easterling, D. R., and T. C. Peterson, 1995: A new method of detecting undocumented discontinuities in climatological time series. *Int. J. Climatol.,* **15,** 369–377.

Enfield, D. B., A. M. Mestas-Nuñez, and P. J. Trimble, 2001: The Atlantic multidecadal oscillation and its relation to rainfall and river flows in the continental U.S. *Geophys. Res. Lett.,* **28,** 2077–2080.

Fritts, H. C., 1976: *Tree Rings and Climate.* Academic Press, 567 pp.

Fye, F. K., D. W. Stahle, and E. R. Cook, 2003: Paleoclimatic analogs to twentieth-century moisture regimes across the United States. *Bull. Amer. Meteor. Soc.,* **84,** 901–909.

Gedalof, Z., and D. J. Smith, 2001: Interdecadal climate variability and regime-scale shifts in Pacific North America. *Geophys. Res. Lett.,* **28,** 1515–1518.

Graumlich, L. J., M. F. J. Pisaric, L. A. Waggoner, J. S. Littell, and J. C. King, 2003: Upper Yellowstone River flow and teleconnections with Pacific basin climate variability during the past three centuries. *Climatic Change,* **59,** 245–262.

Gray, S. T., 2003: Long-term climate variability and its implications for ecosystems and natural resource management in the Central Rocky Mountains. Ph.D. dissertation, University of Wyoming, Laramie, WY, 130 pp.

——, J. L. Betancourt, C. L. Fastie, and S. T. Jackson, 2003: Patterns and sources of multidecadal oscillations in drought-sensitive tree-ring records from the central and southern Rocky Mountains. *Geophys. Res. Lett.,* **30,** 1316, doi:1029/2002GL016154.

Grissino-Mayer, H. D., 1996: A 2129-year reconstruction of precipitation for northwestern New Mexico, U.S.A. *Tree Rings, Environment and Humanity,* J. S. Dean, D. M. Meko, and T. W. Swetnam, Eds., The University of Arizona, 191–204.

Hidalgo, H. G., and J. A. Dracup, 2003: ENSO and PDO effects on hydroclimatic variations in the Upper Colorado River Basin. *J. Hydrometeor.,* **4,** 5–23.

Hirschboeck, K. K., 1991: Climate and floods. National Water Summary 1988–1989—Floods and Droughts: Hydrologic Perspectives on Water Issues, U.S. Geological Survey Water Supply Paper 2375, 67–88.

Holmes, R. L., 1983: Computer-assisted quality control in tree-ring dating and measurement. *Tree-Ring Bull.,* **43,** 69–95.

Hughes, M. K., and L. J. Graumlich, 1996: Drought frequency in central California since 101 B.C. recorded in giant sequoia tree rings. *Climate Dyn.,* **6,** 161–167.

Jain, S., C. A. Woodhouse, and M. P. Hoerling, 2002: Multidecadal streamflow regimes in the interior western United States: Implications for the vulnerability of water resources. *Geophys. Res. Lett.,* **29,** 2036, doi:1029/2001GL014278.

Mann, M. E., and J. Lees, 1996: Robust estimation of background noise and signal detection in climatic time series. *Climatic Change,* **33,** 409–445.

Mantua, N. J., S. R. Hare, Y. Zhang, J. M. Wallace, and R. C. Francis, 1997: A Pacific interdecadal climate oscillation with impacts on salmon production. *Bull. Amer. Meteor. Soc.,* **78,** 1069–1079.

Martner, B. E., 1986: *Wyoming Climate Atlas.* University of Nebraska Press, 432 pp.

McCabe, G. J., and M. D. Dettinger, 1999: Decadal variations in the strength of ENSO teleconnections with precipitation in the western United States. *Int. J. Climatol.,* **19,** 1069–1079.

——, M. A. Palecki, and J. L. Betancourt, 2004: Pacific and Atlantic Ocean influences on multidecadal drought frequency in the United States. *Proc. Natl. Acad. Sci.,* **101,** 4136–4141.

Mock, C. J., 1996: Climatic controls and spatial variations of precipitation in the western United States. *J. Climate,* **9,** 1111–1125.

Muhs, D. R., T. W. Stafford, J. B. Swinehart, S. D. Cowherd, S. A. Mahan, C. A. Bush, R. F. Madole, and P. B. Maat, 1997: Late Holocene eolian activity in the mineralogically mature Nebraska Sand Hills. *Quat. Res.,* **48,** 162–176.

Palmer, W. C., 1965: Meteorological drought. Weather Bureau Research Paper 45, 58 pp.

Richman, M. B., 1986: Rotation of principal components. *J. Climatol.,* **6,** 293–335.

Stahle, D. W., and M. K. Cleaveland, 1988: Texas drought history reconstructed and analyzed from 1698–1980. *J. Climate,* **1,** 59–74.

——, and Coauthors, 1998: Experimental dendroclimatic reconstruction of the Southern Oscillation. *Bull. Amer. Meteor. Soc.,* **79,** 2137–2152.

——, E. R. Cook, M. K. Cleavland, M. D. Therrell, D. M. Meko, H. D. Grissino-Mayer, E. Watson, and B. H. Luckman, 2000: Tree-ring data document 16th century megadrought over North America. *Eos, Trans. Amer. Geophys. Union,* **81,** 121–125.

Stockton, C. W., and D. M. Jacoby, 1976: Long-term surface water supply and streamflow levels in the upper Colorado River Basin. Lake Powell Research Bull. 18, Institute of Geophysics and Planetary Physics, University of California, Los Angeles, Los Angeles, CA, 70 pp.

Stokes, M. A., and T. L. Smiley, 1968: *An Introduction to Tree-Ring Dating.* University of Chicago Press, 73 pp.

Swetnam, T. W., M. A. Thompson, and E. K. Sutherland, 1985: Using dendrochronology to measure radial growth of defoliated trees. Agriculture Handbook 639, USDA Forest Service, 39 pp.

Villalba, R., R. D. D'Arrigo, E. R. Cook, G. C. Jacoby, and G. Wiles, 2001: Decadal-scale climatic variability along the extratropical western coast of the Americas: Evidence from tree-ring records. *Interhemispheric Climate Linkages,* V. Markgraf, Ed., Academic Press, 155–172.

Wigley, T., K. Briffa, and P. D. Jones, 1984: On the average value of correlated time series, with applications in dendroclimatology and hydrometeorology. *J. Climate Appl. Meteor.,* **23,** 201–213.

Woodhouse, C. A., 2001: A tree-ring reconstruction of streamflow for the Colorado Front Range. *J. Amer. Water Resour. Assoc.,* **37,** 561–569.

——, and J. T. Overpeck, 1998: 2000 years of drought variability in the central United States. *Bull. Amer. Meteor. Soc.,* **79,** 2693–2714.

Wyoming Water Development Commission, cited 2003: Wyoming state water plan. [Available online at http://waterplan.state.wy.us/basins/7basins.html.]